

December 1979

LRP 159/79

INVESTIGATION OF THE MODE STRUCTURE IN
THE UNSTABLE RESONATOR OF AN OPTICALLY-
PUMPED FIR LASER

M.R. Siegrist, M.R. Green, P.D. Morgan
and R.L. Watterson

Investigation of the Mode Structure in the Unstable
Resonator of an optically-pumped FIR laser

M.R. Siegrist, M.R. Green, P.D. Morgan and R.L. Watterson*

Centre de Recherches en Physique des Plasmas

Association Euratom - Confédération Suisse

Ecole Polytechnique Fédérale de Lausanne

21, Av. des Bains, CH-1007 Lausanne, Switzerland

ABSTRACT

In this paper we investigate the mode structure in an unstable optically-pumped FIR oscillator as function of the pump beam uniformity. It is shown that the effective output coupling is sensitively dependent on the pump beam intensity profile and the degree of saturation. As example a telescopic D_2O resonator of nominally 75% output coupling is discussed. The mode structure varies from a stable configuration with zero loss in the small signal range to saturated intensity distributions with output coupling factors exceeding the geometrical value.

* Now at Francis Bitter National Magnet Laboratory
Massachusetts Institute of Technology
170 Albany Street, Cambridge, MA 02139 / USA

1. INTRODUCTION

The use of an unstable resonator with lasers in general and optically-pumped FIR lasers in particular has two main advantages: (1) its mode volume is predominantly defined by the resonator geometry and can therefore be easily matched to the size of the gain medium and (2) transverse mode discrimination is quite efficient. Powerful optically-pumped FIR lasers are currently under development with the aim of using them for diagnostic purposes in large plasma machines.¹ In this application it is essential to operate the laser in a single longitudinal mode which represents a limiting factor for the resonator length. Hence, best use of the inverted gain medium has to be made in order to achieve the high powers necessary for a scattering experiment. The unstable resonator configuration suggests itself as an ideal solution.

Usually a FIR oscillator is axially pumped. One possibility of introducing the pump beam into the resonator is from the side by means of a FIR-transmitting reflector (e.g. quartz). With this pump beam reflector set at Brewster's angle for the FIR, the additional resonator roundtrip losses introduced are negligible. Alternatively, axial pumping can be achieved through one of the mirrors, if this mirror is a reststrahlen reflector.² In either case, axial pumping

results in a radially-varying gain profile, reflecting the intensity distribution in the pump beam. The effect of this nonuniform pumping on the unstable resonator modes will be investigated in this paper.

The theoretical understanding of unstable resonators is well developed.³ Modes of the resonator can be obtained as eigenvalue solutions of the equation for beam propagation in its integral (Huygens) form by imposing the condition that the intensity distribution of a mode has to reproduce itself exactly after one roundtrip in the resonator. The equation is usually solved by an interactive process.⁴ The main disadvantage of this method is the fact that it is difficult to include non-uniformities of the gain medium.

Another method of studying unstable resonators with nonuniform gain distribution is by numerical solution of the paraxial wave equation^{5,6,7}. An initially plane wave is propagated repeatedly through the resonator. A mode of the resonator is obtained if the procedure converges. In this way, transient effects can be studied and non-uniform gain profiles can easily be included.

2. MATHEMATICAL FORMULATION

The computational method we use has been developed to study diffraction effects in the design of high-power laser systems⁸ and later on has also been applied to unstable resonators.⁵ The equation that describes the propagation of electromagnetic radiation through a medium with dielectric constant ϵ , in terms of the time-independent electric field U , is

$$\nabla^2 U + k^2 \epsilon U = 0. \quad (1)$$

We remove the fast phase variation by defining $U = E e^{ikz}$, neglecting second order derivatives along the z -axis and define

$$\epsilon = 1 - i g/k \quad (2)$$

with an intensity gain coefficient g (changes of refractive index are not considered in this paper). This gives

$$\nabla^2 E + 2ik \frac{\partial E}{\partial z} - ikgE = 0. \quad (3)$$

This equation, rewritten for cylindrical geometry, i.e.

$$\frac{1}{r} \frac{\partial}{\partial r} \left(r \frac{\partial E}{\partial r} \right) + 2ik \frac{\partial E}{\partial z} - ikgE = 0 \quad (4)$$

is solved numerically with the difference scheme described in⁹, slightly modified to include the gain term. The difference equation is implicit and centered in z , thus producing stable solutions in which energy conservation is maintained.

The mirrors are assumed to be 100% reflecting and hence only change the phase distribution of the wave front. A mirror with radius of curvature R can be described by a multiplication factor $\exp(ikr^2/R)$, where r is the distance from axis.

Numerically this phase shifting can lead to problems related to the non-uniqueness of trigonometric functions. One has to make sure that the phase variation from one radial grid point to the next does not exceed π , otherwise the information on the phase front curvature is lost between axial steps.⁵ This condition is automatically checked in our code and changes are made, if necessary, to see that it is satisfied.

As a test of our code we investigated a stable confocal resonator where the intensity distribution of the fundamental mode and the beam caustic are well known.¹⁰ The correct intensity distribution was reproduced after one round-trip and the caustic showed the correct shape.

3. EDGE DIFFRACTION OF OUTPUT COUPLER

In unstable telescopic resonators a slight problem arises due to the sharp edge of the small mirror which produces pronounced diffraction effects. A discontinuity in the intensity distribution cannot be handled adequately with our numerical procedure. We find that numerical instabilities develop before the procedure has converged to a reproducible intensity distribution. We avoid this problem, which has been discussed in detail in⁵, in the usual way: by slightly apodizing the mirror edge. We smoothly truncate the intensity reflection coefficient $R(r)$ of a mirror of radius r_0 by a function of the following form

$$R(r) = \left[1 + \exp((r - r_0)/d) \right]^{-1} \quad (5)$$

This function has been proposed by Hadley⁹ as a convenient, but by no means unique, way of smoothing out sharp edges. The apodization parameter d determines the steepness of the smoothed edge. In Fig. 1 we show the reflection profile of a mirror for the d -value of 0.005 mainly used in this paper. It is seen that the transition region from the fully-reflecting mirror surface of 5 cm diameter to zero reflection extends over a radial distance of less than $\frac{1}{2}$ mm.

We do not propose to use tapered mirrors in an actual experiment and hence we have to investigate the effect of this mathematical smoothing. In Fig. 2, we show intensity profiles obtained from a circular aperture of 5 cm diameter, illuminated with a plane wave and observed at a distance of 1m. The wavelength is 66 μm , resulting in a Fresnel number $N = r_0^2 / (z\lambda)$ of 9.47. The top curve in Fig. 2 shows the intensity profile for an aperture with a sharp edge and the bottom curve shows the results for an apodized aperture with an apodization parameter $d = 0.01$. The left halves of the profiles represent calculations with our differential method for step sizes of 200 in axial and radial direction, whereas on the right we display solutions of the integral equation.¹¹

The following observations are made: (1) the further away from the axis the better the agreement, (2) there is a correspondence between the number of rings and their positions on either side, (3) the shapes of the outer rings on either side are similar, but the inner rings, and especially the central spike, differ.

From additional runs the following supplementary information was obtained: the height of the central spike (or depression, depending on Fresnel number) and the shape of the innermost ring depend on the radial and axial step sizes. The agreement does not

necessarily improve with finer resolution. Both methods show that the central features depend very sensitively on the edge of the aperture.

The inability to correctly reproduce the central features with a numerical procedure based on equation (4) is partly due to the discontinuity in the initial intensity distribution and partly to the omitted second order term $\frac{\partial^2 E}{\partial z^2}$. The discontinuity is smoothed out in the first few axial steps in a way which is characteristic of the axial step size. This explains the observed dependence of the center intensity on step size. In the case of a hard aperture the intensity on axis should disappear whenever $N = r_0^2/(z\lambda)$ is an even number and reach large values in between. This fast oscillation is not compatible with the assumption of a slowly varying axial intensity, which was made to justify neglecting $\frac{\partial^2 E}{\partial z^2}$.

We conclude that our approach is not very suitable to study diffraction effects of hard apertures, but quite accurate for smoothed out edges. We demonstrate this by showing in Fig. 3 the deviation of the intensity profile from the hard aperture profile for various apodizing parameters d and for both integral and differential methods of calculation. As a measure of the deviation of the profiles we plotted the sum of the squares of the differences of all calculated intensity points from their corresponding hard aperture values. While the profiles obtained from the integral method

smoothly approach the hard aperture case, the accuracy of the differential method also improves with decreasing d , but is always limited. However, up to d -values of ~ 0.01 no significant additional loss in accuracy is incurred. What is mainly affected by slight apodization is the high frequency ripple (see Fig. 2) which is not correctly represented anyhow.

Experimentally one observes quite smooth intensity profiles exiting from unstable resonators of CO_2 lasers, for example.¹² This indicates that some apodization occurs even in the case of a hard aperture output coupler. This can be due to small mechanical irregularities of the mirror edge, slight misalignment of the mirrors or imperfections of the gain medium such as laser-induced medium perturbation in pulsed CO_2 lasers.^{13,14} For several of the calculations reported in the following section, control runs have been performed with different apodization parameters. Differences are usually below 5%.

4. GAIN SATURATION

The saturation behaviour in an optically-pumped far infrared laser depends in a complicated way on both the far infrared and the pump intensities and on the degree of coincidence between pump and absorption line. The theory of this interaction has been developed

by Panock and Temkin.¹⁵ While it allows one to model in detail the pump beam absorption and its saturation, it does not account for interference effects between the forward and backward propagating beams in the resonator.

An expression for gain saturation which includes this mechanism has recently been given by Agrawal and Lax.¹⁶ It was not derived specifically for optically-pumped lasers but is applicable to situations where the effect of pump beam absorption can be neglected. The gain g_f in the forward direction according to eq. (8) of ref.¹⁶ can be written as

$$g_f = \frac{g_o(1 + i\Omega)}{(a^2 - b^2)^{\frac{1}{2}}} \left(1 - \frac{a - (a^2 - b^2)^{\frac{1}{2}}}{2 I_f}\right) \quad (6)$$

$$\text{with } a = 1 + \Omega^2 + I_f + I_b$$

$$b = 2 (I_f \cdot I_b)^{\frac{1}{2}}$$

where I_f , I_b are the beam intensities in the forward and backward directions and Ω the frequency offset expressed in linewidths. The above expression (with $\Omega = 0$) was used in the code for the results presented in Fig. 4. I_b is obtained from the stored intensity distribution of the previous pass through the resonator.

5. RESULTS

We investigated the effective reflectivity of the output coupler in a telescopic unstable resonator as a function of the pump beam profile. The FIR gain medium is D_2O vapour pumped with the 9P(32) line of a CO_2 laser, resulting in an output at $66 \mu m$ wavelength. In the resonator chosen as example, the convex output coupler of 5 cm diameter and 2 m radius of curvature faces a 10 cm diameter concave mirror of 4 m radius of curvature at a distance of 1 m. Geometrically the reflectivity of the output coupler is therefore 25%.

We assume a Gaussian gain profile resulting from a pump beam with Gaussian intensity distribution and define a pump uniformity parameter η as the ratio of the $1/e$ full width of the gain profile to the diameter of the small mirror. Starting with a plane wave of flat intensity distribution, convergence to a stable mode structure is usually obtained after ~ 6 roundtrips. We define as "effective reflectivity" of a mirror the ratio of the total reflected intensity to the total incident intensity. The effective reflectivity is thus not only mirror, but also mode, dependent.

In Fig. 4 we plot the effective reflectivity of the output coupler versus axial gain coefficient for several values of η and for the small signal and saturated gain regimes. We find that the

effective reflectivity of the output coupler increases rapidly with gain for nonsaturating intensities and even approaches 100%. It is to be expected that a beam propagating in a medium with Gaussian gain profile will decrease in beam width since rays close to the axis experience a higher gain than those further out. This is illustrated in Fig. 5 where we plot the beam halfwidth of a plane wave with an initially-flat intensity distribution propagating according to geometrical optics laws through a medium with Gaussian gain profile for three different axial gain values. Since diffraction is neglected in this case the beam shrinks continuously. With the counteracting effect of diffraction, however, a steady-state profile develops, as in the unstable resonator considered above.

If the width of the steady-state profile on the small mirror is less than the mirror diameter, no further output coupling occurs. In the saturated regime the gain profile is flattened and the effect much less pronounced. In fact, for larger values of the pump uniformity parameter η the effective reflectivity of the output coupler can even be lower than its geometrical value. This is due to the fact that in the region centered around the axis the diverging forward and parallel backward propagating beams overlap, resulting in higher average intensities and hence more heavily saturated gain, whereas in the outer region the two beams only overlap in the vicinity of the larger mirror.

For illustration we depict in Fig. 6 the computed small signal and saturated intensity distributions inside the resonator for a small signal gain of $2\% \text{ cm}^{-1}$ and a pump beam uniformity parameter of $\eta = 1$. A large d-value of 0.1 was chosen in this case to suppress diffraction effects which are irrelevant in this context.

In connection with the results presented in Fig. 4 we also investigated the way in which detuning and interference between the backward and forward propagating waves affect saturation and, hence, beam profiles in the resonator. The standard way of treating saturation without accounting for interference effects or detuning is by means of

$$g = g_0 \frac{1}{1 + I} \quad (7)$$

where I is the sum of the beam intensities in forward and backward direction. We recalculated the curve for $\eta = 2$ in Fig. 4 with the above gain equation. It follows the displayed curve very closely, with reflection values of $\frac{1}{2}$ to 1% higher. The steady-state beam profiles immediately in front of the output coupler are shown in Fig. 7 for the two different ways of treating saturation. The main difference is that a slightly more structured profile is obtained if interference effects are included. In both curves the right half shows the profile one roundtrip later than the left half, indicating in this way the degree of convergence obtainable.

While beam profiles are not significantly influenced by interference effects, the power coupled out of the oscillator drops by about 15%. This is illustrated in Fig. 8 which shows the steady-state output power (in arbitrary units) as a function of the small-signal gain coefficient. The power increase with more uniform pumping reflects the higher output coupling as well as the higher average gain coefficient resulting from normalizing the gain on axis rather than its average over the resonator diameter. Output power increases linearly with small signal gain as expected for saturated conditions.

We have also performed some calculations on the effect of detuning, the results of which are presented in Table I. Again we observe very little change in the intensity distribution inside the resonator, but the total power coupled out of the oscillator decreases with increasing detuning.

The difference in effective output coupling in the small signal and saturated gain regimes can have important consequences. Consider a pump pulse which rises on a time scale consistent with several tens of roundtrips in the FIR oscillator. Initially, the gain will be small and output coupling will be close to the geometrical value. A mode structure develops from noise. The gain now rises and so does the effective reflectivity of the output coupler, resulting in a high resonator q -value. The FIR intensity builds up rapidly, but

practically no output is obtained during this phase. Due to the fast buildup of FIR intensity and the increasing gain resulting from the continuously-growing pump intensity, saturation is approached quite suddenly. The mode structure changes, the effective reflectivity of the output coupler drops and output is obtained. The effect is similar to passive Q-switching, resulting in a fast rising pulse. The exact dynamic behaviour is complex and depends on pump pulse shape and time delays for convergence to a new mode structure.

For a temporally-stationary pump beam of Gaussian intensity distribution ($\eta = 1$) we investigated the change of the effective reflectivity of the output coupler and the power coupled out of the resonator and compare them with the values calculated for a uniformly-pumped oscillator. We assume that the small-signal far-infrared gain is proportional to the pump intensity. To obtain comparable conditions we adjust the intensity of the uniform pump beam so that the intensities integrated over the oscillator cross-section (size of concave mirror) are identical in both cases.

The results are presented in Fig. 9, where the buildup from a flat intensity profile of intensity 10^{-8} times saturation intensity is shown. We observe indeed a faster rising output pulse occurring earlier in the case of a non-uniform pump-beam profile. While the effective reflectivity of the output coupler is practically constant in the uniformly-pumped resonator, it drops to almost half its small signal value during transition to saturation in the case of the

Gaussian gain distribution. Convergence to a steady-state intensity profile is observed after ~ 5 roundtrips in the small signal region. During this period R_{eff} fluctuates around its steady-state value (55% in curve (a)).

To illustrate the change of the beam profile during the transition from nonsaturating to saturating intensities we show in Fig. 10 the calculated profiles immediately in front of the output coupler for consecutive roundtrips. The units of intensity are arbitrary and different for each curve. While there is not much change in the beam profile for uniform pumping (apart from diffraction effects) a considerable broadening and flattening is observed during transition to saturating intensities in the case of a Gaussian pump beam.

4. CONCLUSIONS

We have shown that the uniformity of the pump intensity profile has a great influence on the mode structure and hence the degree of output coupling in an unstable telescopic FIR resonator which is axially pumped with a CO₂ laser. If Q-switching effects are to be avoided, a flat-topped pump intensity distribution of diameter comparable to that of the larger mirror has to be used. Alternatively, the pump intensity profile can be tailored to achieve some particular type of temporal FIR pulse shape. To what degree this can actually be achieved would have to be shown by experiment or a more comprehensive computer modelling.

This work has been supported by the Swiss National Foundation and Euratom.

FIGURE CAPTIONS

- Fig. 1 Apodized reflection profile of a mirror of 5 cm diameter for the apodization parameter $d = 0.005$ mainly used in this paper.
- Fig. 2 Intensity profiles 1 m behind circular aperture of 5 cm diameter ($\lambda = 66 \mu\text{m}$; $N = 9.47$). Top curve: aperture with sharp edge. Bottom curve: aperture apodized with $d = 0.01$. Left halves (a), (c) show results of differential method, right halves (b), (d) show results of integral equation.
- Fig. 3 Deviation of intensity profiles from sharp edge case for different apodization parameters d , for conditions defined in Fig. 2.
- Fig. 4 The effective reflection of the output coupler as function of the small signal gain, for small (ss) and saturating (sat) intensities. The parameter η is the quotient of the 1/e full width of the Gaussian gain profile and the small-mirror diameter ($\eta = \infty$: flat intensity distribution). The resonator parameters are shown in Fig. 6.

Fig. 5 The beam diameter $2 w_0$ of an initially plane wave of flat intensity distribution propagating in a medium with a Gaussian gain profile of halfwidth $2 r_0$ for 3 different axial gain coefficients g_0 , as obtained from geometrical optics considerations (no diffraction).

Fig. 6 Intensity profiles in forward (I_f) and backward (I_b) direction for 5 axial positions in an unstable resonator for the saturating (a) and small signal (b) gain regimes. Axial gain $g_0 = 0.02 \text{ cm}^{-1}$; $\eta = 1$. Also shown are the beam caustics in the resonator for forward and backward propagating beams (c).

Fig. 7 Intensity profiles in front of output coupler. Top curve with, bottom curve without, consideration of interference effects in gain saturation. In both curves right half shows profile one roundtrip later than left half ($g_0 = 2\% \text{ cm}^{-1}$, $\eta = 2$).

Fig. 8 Steady-state output power as function of axial small signal gain for different gain profiles.
(a) : $\eta = 1$; (b) : $\eta = 2$; (c) : $\eta = 5$
With exception of (b₂) interference effects are included.

Fig. 9 Output intensity (c, d) and effective reflectivity (a, b) of output coupler for a Gaussian (a, c) and a flat (b, d) gain profile.

Fig. 10 Intensity profiles in front of output coupler for consecutive roundtrips. Left: Gaussian gain profile, right: flat profile. (Units of intensity different for each curve.)

REFERENCES

- 1) P.D. Morgan, M.R. Green, M.R. Siegrist, R.L. Watterson,
Plasma Phys. Cont. Fusion, 5, 141-158 (1979).
- 2) M.R. Green, P.D. Morgan, M.R. Siegrist, J. Phys. E: Sci.
Instrum 11, 1-2, (1978).
- 3) A.E. Siegman, Appl. Optics 13, 353-367, (1974).
- 4) D.B. Rensch, A.N. Chester, Appl. Optics 12, 997-1010, (1973).
- 5) D.B. Rensch, Appl. Optics 13, 2546-2561, (1974).
- 6) M. Lax, G.P. Agrawal, W.H. Louisell, Optics Letters 4,
303-305, (1979).
- 7) E.A. Sziklas, A.E. Siegman, Appl. Optics 14, 1874-1889,
(1975).
- 8) A.J. Campillo, J.E. Pearson, S.L. Shapiro, N.J. Terrel jr.,
Appl. Phys. Lett. 23, 85-87, (1973).

- 9) G.R. Hadley, IEEE J. of Quantum Electronics, QE-10, 603-608, (1974).
- 10) H. Kogelnik, T. Li, Appl. Optics 5, 1550-1567, (1966).
- 11) Laser Handbook, vol. 1, F.T. Arecchi, E.O. Schulz-Dubois, North-Holland 1972, Amsterdam, pg 165.
- 12) R.J. Freiberg, P. Chenausky, C.J. Buczek, IEEE J. Quantum Electron. QE-8, 882 (1972).
- 13) V. Yu. Baranov, S.A. Kazsakov, D.D. Malyuta, V.S. Mezhevov, A.P. Napartovich, V.G. Nisiev, M. Yu. Orlov, A.I. Starodubtsev, and A.N. Starostin, Appl. Optics 19, 930-936, (1980).
- 14) V.G. Roper, H.M. Lamberton, E.W. Parcell, A.W.J. Manley, Opt. Commun. 25, 235-240, (1978).
- 15) R.L. Panock, R.J. Temkin, IEEE J. of Quantum Electronics QE-13, 425-434, (1977).
- 16) G.P. Agrawal, M. Lax, J. Opt. Soc. Am. 69, 1717-1719, (1980).

Table 1 : The effect of detuning

detuning parameter	eff. reflection (%)	output (arb. units)
Ω		
0	27.3	55
$\frac{1}{2}$	27.7	49
1	28.7	37.5
2	29.1	\sim 14

These results are based on an axial small-
signal gain of $2\% \text{ cm}^{-1}$ and a pump beam uni-
formity parameter $\eta = 2$

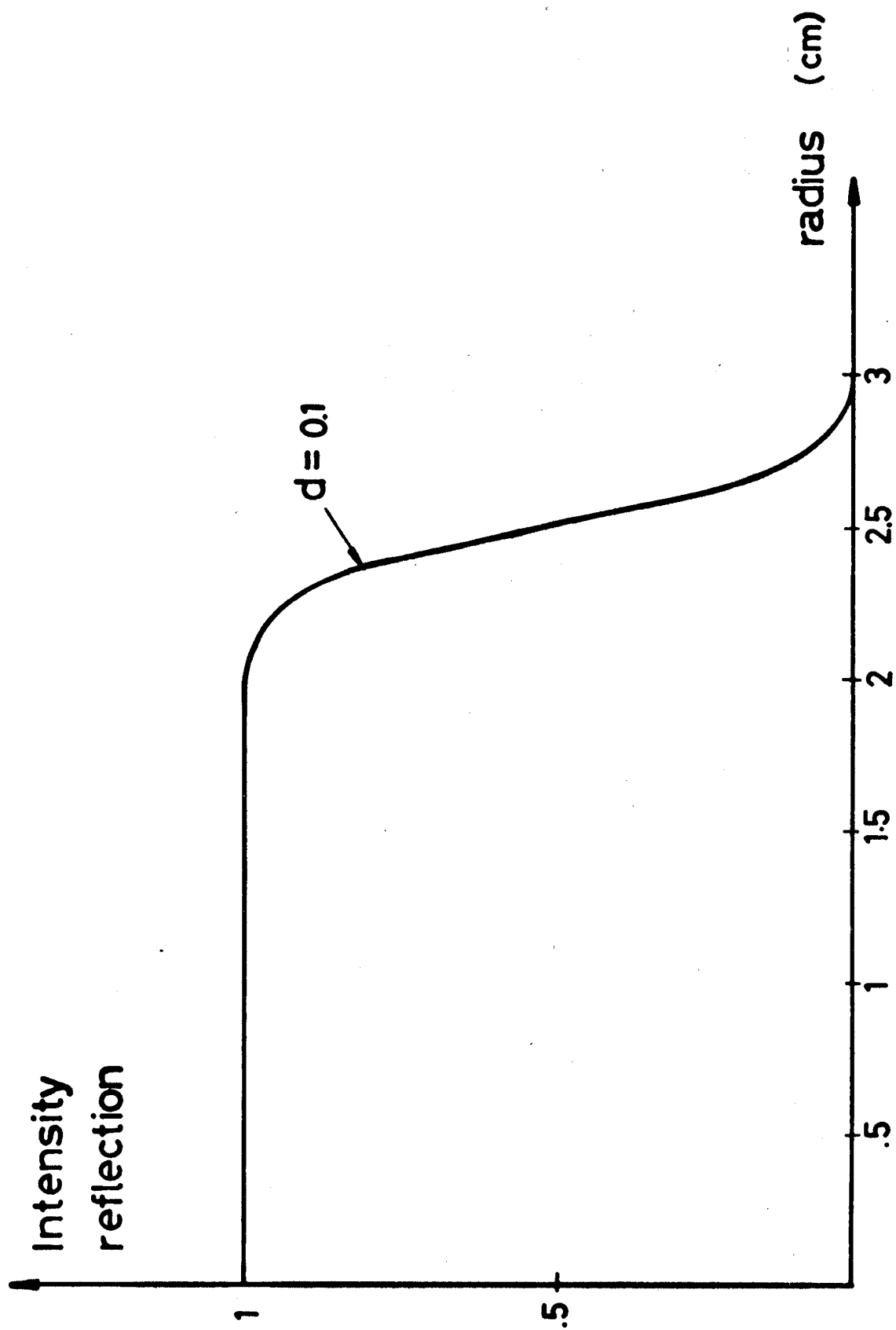


FIG.1

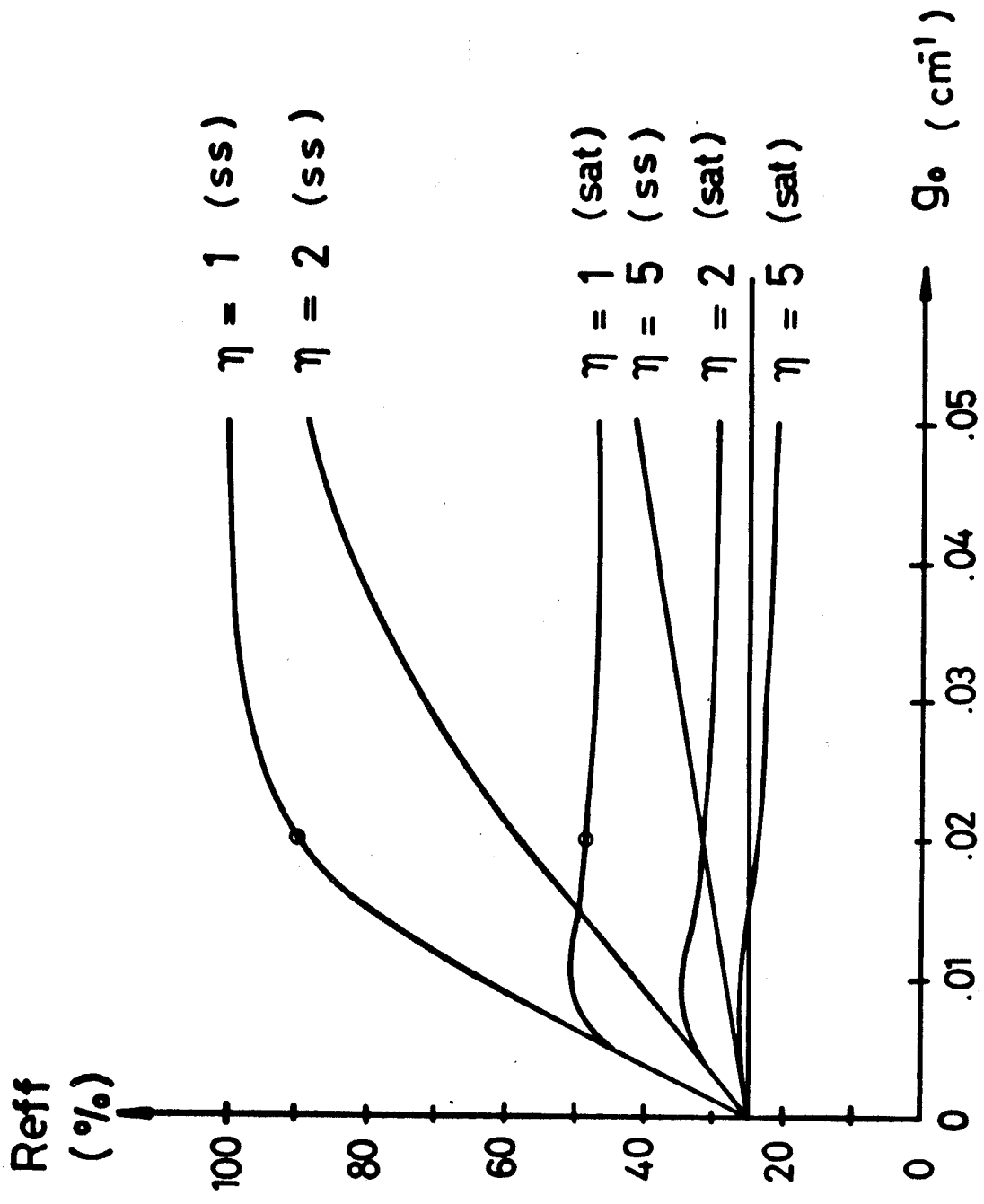


FIG.2

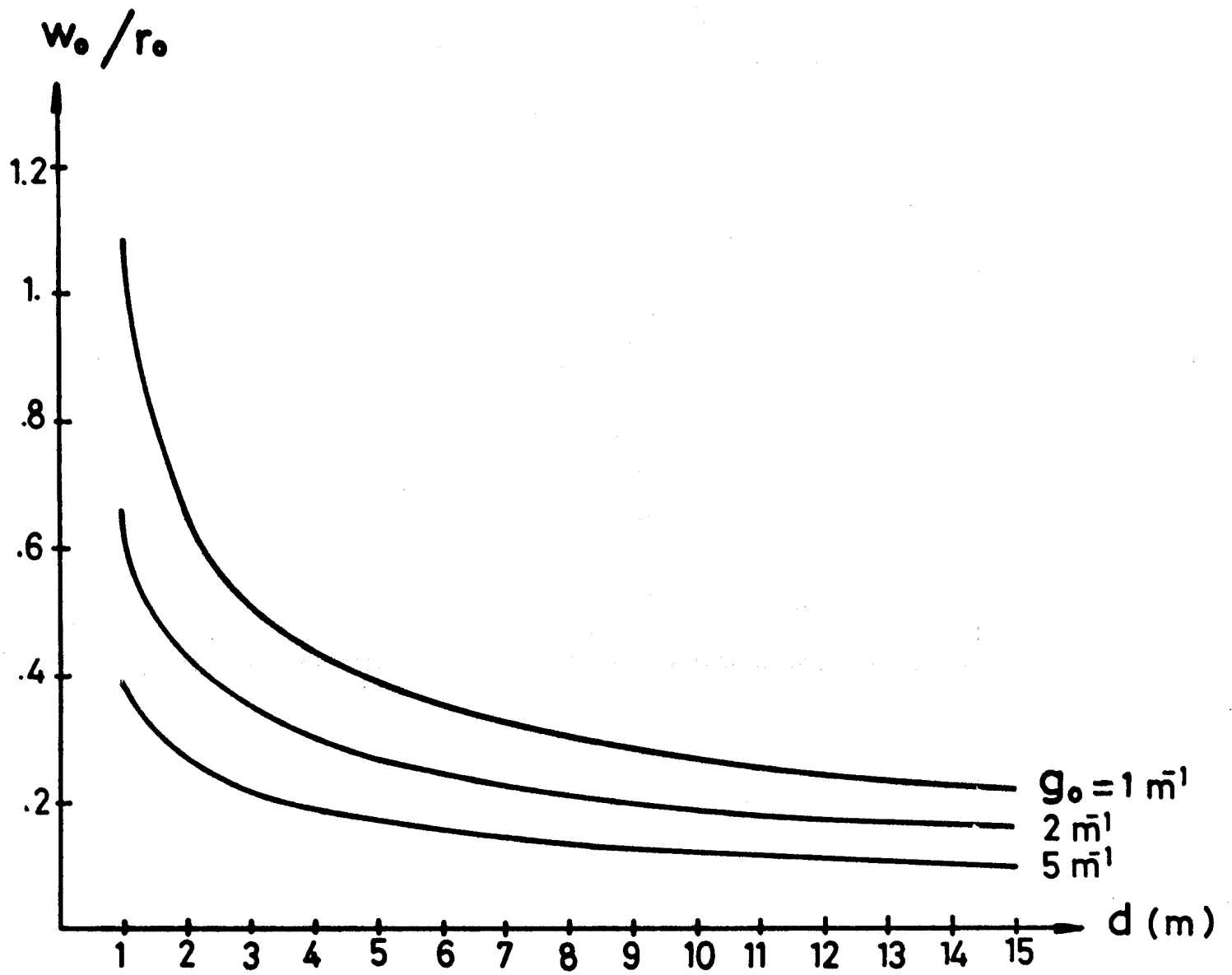


FIG.3

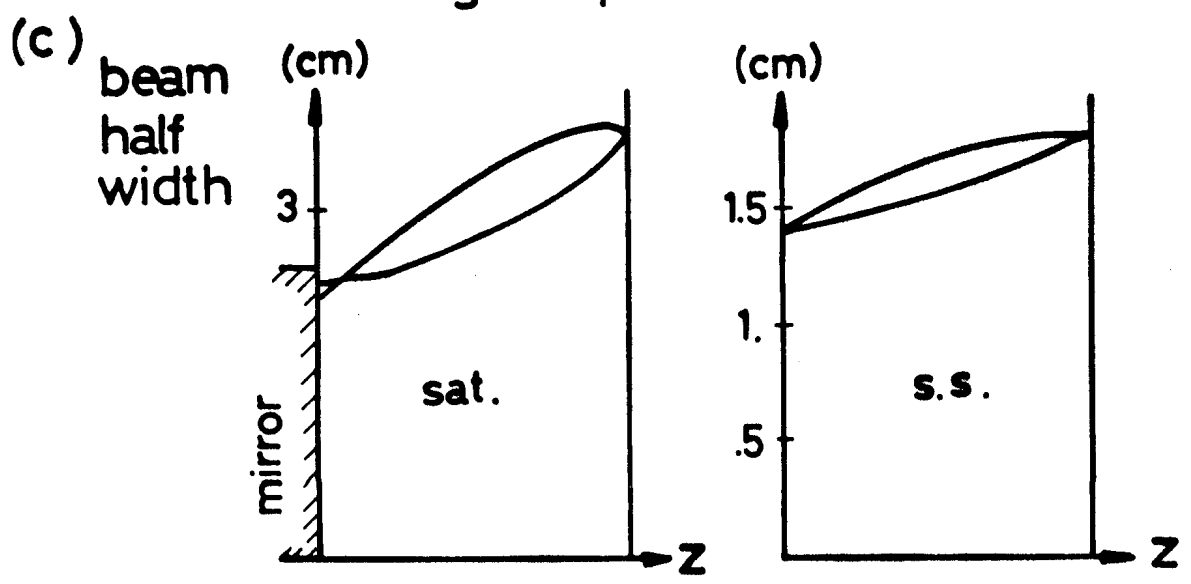
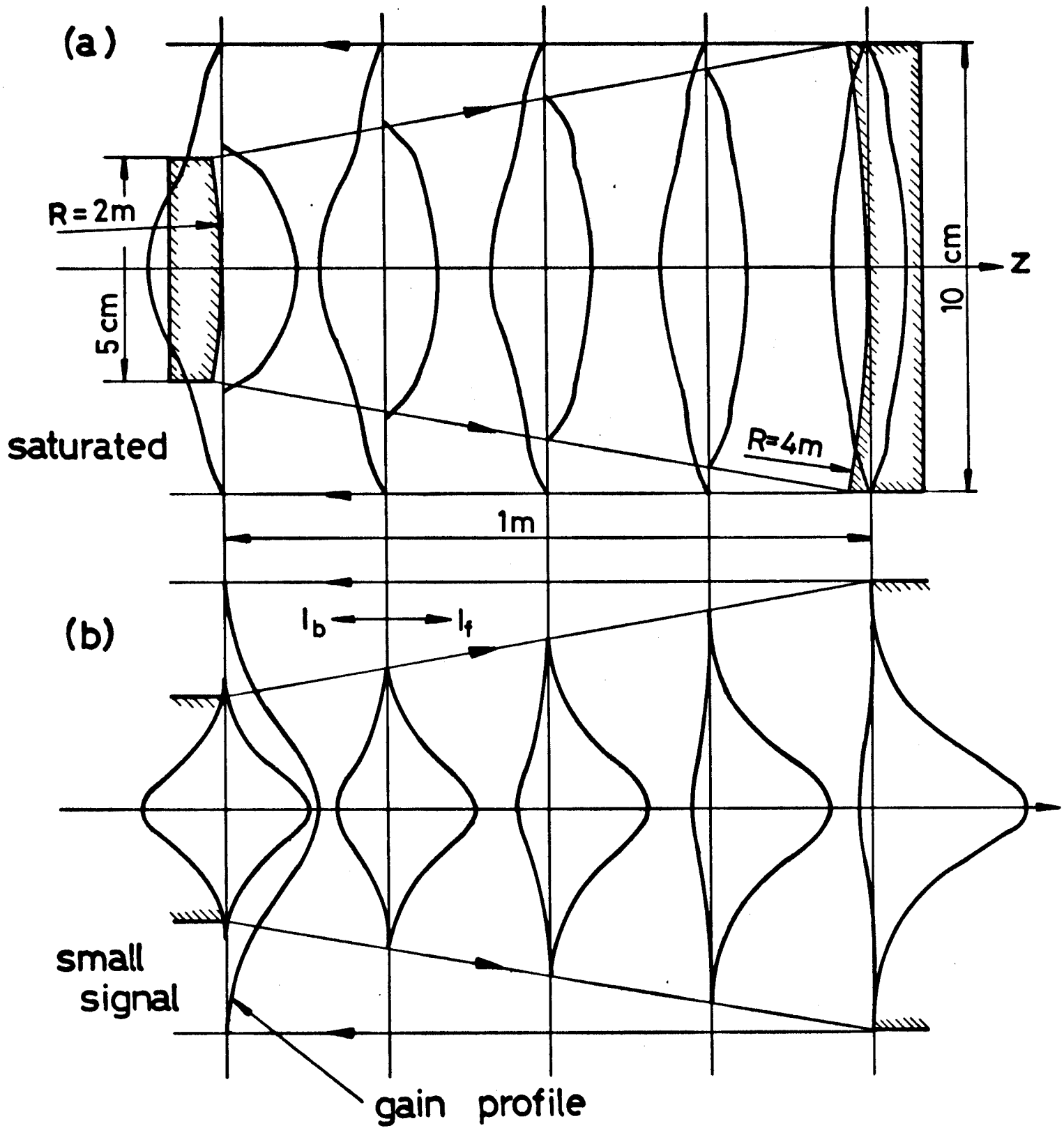


FIG.4